ISSN 1062-8738, Bulletin of the Russian Academy of Sciences: Physics, 2017, Vol. 81, No. 1, pp. 43–46. © Allerton Press, Inc., 2017.
Original Russian Text © A.G. Balanov, A.A. Koronovskii, O.I. Moskalenko, A.O. Selskii, A.E. Khramov, 2017, published in Izvestiya Rossiiskoi Akademii Nauk, Seriya Fizicheskaya, 2017, Vol. 81, No. 1, pp. 50–54.

Effect of the Form and Localization of Doping Density Perturbations on the Current Characteristics in a Semiconductor Superlattice

A. G. Balanov[b, c], A. A. Koronovskii[a], O. I. Moskalenko[a], A. O. Selskii[a, b, *], and A. E. Khramov[b]

[a] *Saratov State University, Saratov, 410012 Russia*
[b] *Saratov State Technical University, Saratov, 410054 Russia*
[c] *Department of Physics, Loughborough University, LE11 3TU Loughborough, United Kingdom*
**e-mail: feanorberserk@gmail.com*

Abstract—The effect doping density perturbations have on the current characteristics in a semiconductor superlattice is studied. The current characteristics are shown to depend on the localization and form of the perturbation. The effect of perturbations is strongest near the superlattice emitter. The effect grows along with the density profile integral and depends weakly on the form of the profile.

DOI: 10.3103/S1062873817010063

INTRODUCTION

Semiconductor superlattices are very complex nanostructures that consist of several alternating thin (about 10 nm) layers of different semiconductor materials [1, 2]. These structures are used to study various quantum-mechanical effects related to resonant tunneling and Bloch oscillations; they are also a unique testing field for studying and understanding the processes of physics of condensed matter [3, 4]. In addition, ultrafast Bloch oscillations and spatiotemporal electronic structures called domains (in analogy with the domains in a Gunn diode [5, 6] that occur when a dc voltage is applied to a superlattice) make the latter a promising element for the generation, amplification, and detection of high-frequency (up to several THz) signals. The transmission of domains through a semiconductor superlattice leads to the generation of an oscillating current flowing through the structure. Researchers today are increasingly interested in studying electron transport through semiconductor superlattices in terms of nonlinear dynamics, which allows them to observe and explain different effects in a system [7–11].

It is well known that electron transport in a superlattice is affected by the density of doping on the collector and emitter [12], or directly in the structural layers [13, 14]. In this work, we investigate how inhomogeneities in the doping concentration, introduced in the form of local perturbations, affects electron transport in a semiconductor superlattice. In contrast to the random doping density fluctuations in [13, 14], we systematically analyze the effect such perturbation parameters as localization and form have on the characteristics of a current flowing through a semiconductor superlattice, especially the I–V characteristic.

NUMERICAL MODEL

The density of a current flowing through a semiconductor superlattice is determined from the drift approximation [2, 9]

$$J = env_d(\overline{F}). \tag{1}$$

Here, $n(x,t)$ is the electron density, $J(x,t)$ is the current density, $F(x,t)$ is the electric field strength, v_d is the electron drift velocity calculated for the average electric field strength $\overline{F}$, and $e > 0$ is the elementary charge. The dependence of the drift velocity on the electric field strength is determined using the Esaki–Tsu formula [4]. The strength and density can be calculated by solving the Poisson and continuity equations [2, 9]

$$e\frac{\partial n}{\partial t} = -\frac{\partial J}{\partial x}, \qquad \frac{\partial F}{\partial x} = \frac{e}{\varepsilon_0\varepsilon_r}(n - n_{D0}), \tag{2}$$

where t is time and coordinate x corresponds to the direction of electron motion in the semiconductor superlattice. Parameters $\varepsilon_0, \varepsilon_r = 12.5$ correspond to the absolute and relative permittivities, and $n_{D0} = 3\times10^{22}$ m^{-3} is the equilibrium electron density.

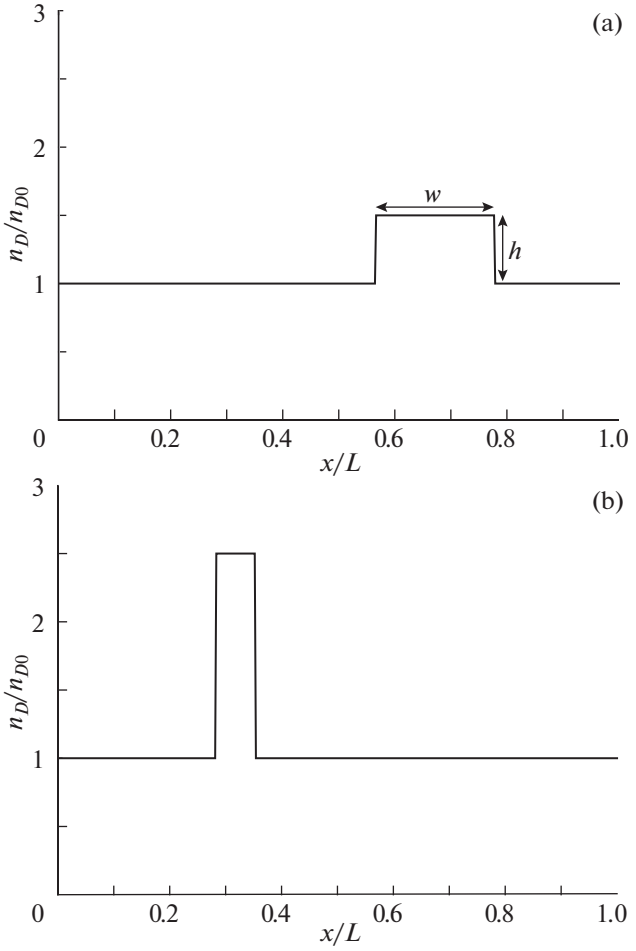

Fig. 1. Doping density profiles. Examples of different perturbation localizations and forms.

The investigated perturbation is a local increase in doping density. To insert the perturbation, we modify Poisson equation (2):

$$\frac{\partial F}{\partial x} = \frac{e}{\varepsilon_0 \varepsilon_r}(n - (n_{D0} + n_{D1}(x))), \quad (3)$$

where $n_{D1}(x)$ is the piecewise linear function

$$n_{D1}(x) = \begin{cases} 0, x < x' - \Delta x \\ h, x' - w/2 < x < x' + w/2. \\ 0, x > x' + \Delta x \end{cases} \quad (4)$$

Here, x' is the position of the perturbation's center, w is the width of the investigated perturbation, and h is its height (the difference from equilibrium density n_{D0}). Doping density profile $n_D(x) = n_{D0} + n_{D1}(x)$ at several values of x', w, and h is shown in Fig. 1. For convenience, the density is normalized to the n_{D0} value; the perturbation center's coordinate, to structure length $L = 116.2$ nm.

CHANGE IN THE LOCALIZATION OF THE DOPING DENSITY PERTURBATION

Let us first consider how the current characteristics (particularly the $I-V$ characteristic) change upon variation in the localization of a perturbation. We fix the perturbation's dimensions by choosing parameters $w = 24.9$ nm ($w/L = 0.10715$) and $h = 1.5\times10^{22}$ m^{-3} ($h/n_{D0} = 0.5$), which correspond to the profile shown in Fig. 1a. To build the $I-V$ characteristic in the part where there are current oscillations, we average the current value in the $I-V$ characteristic over time (the technique for plotting the $I-V$ characteristics and their form for the state of unperturbed doping density ($n_{D1}(x) = 0$ along the superlattice) was described in [11]). Figure 2a shows examples of $I-V$ characteristics for different localizations of the perturbation center (curve *2* corresponds to $x' = 46.5$nm; curve *3*, to $x' = 93$ nm) and when there is no perturbation (curve *1*). We can see that the $I-V$ characteristics change notably with localization. To characterize the variation in the $I-V$ characteristic upon shifting the center of the doping density perturbation, we introduce quantity Θ, calculated as

$$\Theta = \int |I(V) - I_0(V)| dV, \quad (5)$$

where $I(V)$ is the current at a certain voltage for the perturbed state and $I_0(V)$ is the current at a certain voltage for the unperturbed state. The dependence of this quantity on perturbation center's coordinate is presented in Fig. 2b. It can be seen that the Θ values are higher when the perturbation is near the emitter of the heterostrucutre and fall rapidly as the perturbation approaches the superlattice collector. It follows that the behavior of the investigated system depends not only on the presence of a doping density perturbation, but also on its spatial localization.

Another important characteristic of the collective electron behavior is threshold voltage V_c of the onset of current oscillations. In the $I-V$ characteristic, this value corresponds to the beginning of the descending portion. The dependence of this quantity on the perturbation center's coordinate is shown in Fig. 2c. It is clearly seen that there is the maximum threshold voltage for the perturbation center's coordinate $x'/L = 0.4$ ($x' = 46.5$ nm). At other spatial localizations of the perturbation, the threshold voltage at which the generation of current oscillations starts is lower.

CHANGE IN THE FORM OF THE DOPING DENSITY PERTURBATION

To study the effect the dimensions of a doping density perturbation have on the current characteristics, we fix spatial localiztion $x'/L = 0.4$($x' = 46.5$ nm) of the perturbation. This value corresponds to the strongest effect on the $I-V$ characteristic of a semiconductor superlattice.

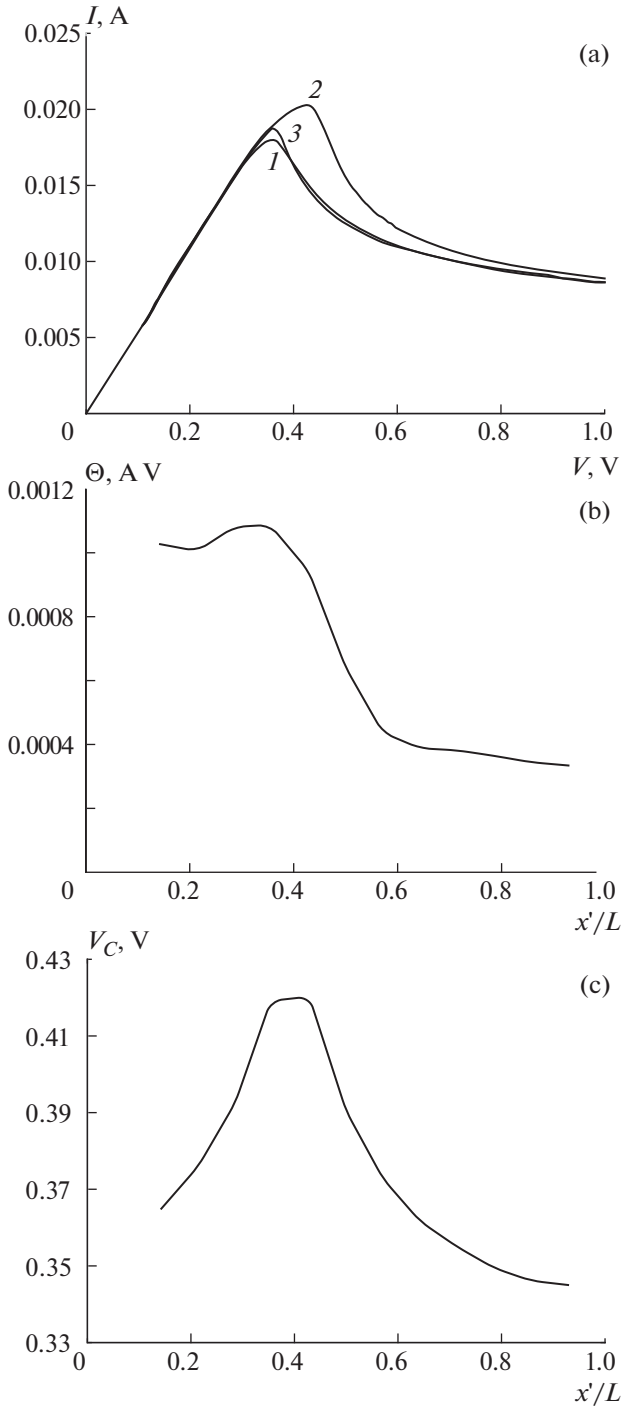

Fig. 2. (a) $I-V$ characteristics for different localizations of a doping density perturbation with fixed form. (b) Dependence of integral quantity Θ on the coordinate of the doping density perturbation's center. (c) Dependence of the threshold voltage at which the generation of current oscillations starts on the coordinate of the doping density perturbation's center.

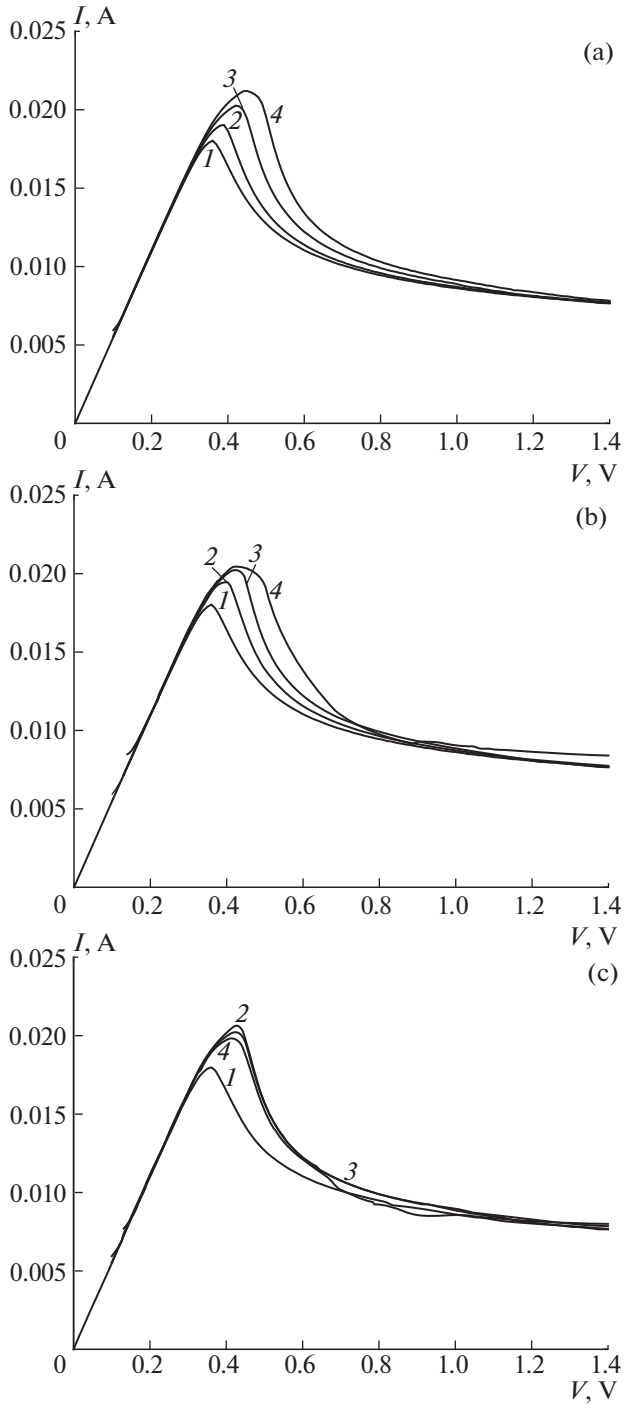

Fig. 3. $I-V$ characteristics for different forms of a doping density perturbation with a fixed perturbation center coordinate (a) as perturbation width w in the doping density profile grows, (b) as perturbation height h in the doping density profile grows, and (c) under the condition $h \times w = \text{const}$. Curve *1* in all of the figures represents the unperturbed doping density.

Figure 3a illustrates the variation in the $I-V$ characteristic as the perturbation grows wider at a fixed height of $h = 1.5 \times 10^{22}$ m^{-3}. The figure shows $I-V$ characteristics for $w = 0$ (unperturbed doping density, curve *1*), $w = 8.3$ nm (curve *2*), $w = 24.9$ nm (curve *3*), and $w = 41.5$ nm (curve *4*). As the perturbation grows

wider, the threshold voltage of the onset of current oscillations increases. The maximum current flowing thorough the structure increases as well.

We now fix doping density perturbation width $w =$ 24.9 nm and gradually raise the perturbation's height. The $I-V$ characteristics are presented in Fig. 3b for $h = 0$ m^{-3} (unperturbed doping density, curve *1*), $h = 0.75\times10^{22}$ m^{-3} (curve *2*), $h = 1.5\times10^{22}$ m^{-3} (curve *3*), and $h = 3\times10^{22}$ m^{-3} (curve *4*). As with the growing width of the doping density perturbation, the threshold voltage of the onset of current generation and the maximum current grow along with the perturbation's height.

Based on these data, we proposed building the $I-V$ characteristics for when variation in the perturbation's width is inversely proportional to the height: $h\times w = \text{const}$. This denotes the invariability of the area of perturbation in the density profile (profile integral) of the dopant upon varying the form of the perturbation. Figure 3 presents the $I-V$ characteristics for the following perturbation parameters: unperturbed doping density (curve *1*), $h = 0.9\times10^{22}$ m^{-3} and $w =$ 41.5 nm (curve *2*), $h = 1.5\times10^{22}$ m^{-3} and $w = 24.9$ nm (curve *3*), and $h = 4.5\times10^{22}$ m^{-3} and $w = 8.3$ nm (curve *4*). It can be seen that with a constant area of perturbation, varying the form has almost no effect on the $I-V$ characteristics.

CONCLUSIONS

The characteristics of oscillations in a current flowing through a superlattice depend on the spatial localization of the doping density perturbation. If the latter is close to the emitter of the superlattice, the $I-V$ characteristic changes significantly. The threshold voltage at which the generation of oscillations starts and the maximum current increase in particular, compared to the unperturbed electron behavior in a superlattice. If we shift the perturbation to the collector of the device, the $I-V$ characteristic appears similar to the unperturbed case.

It was shown that the value of the variation in the characteristics is related to the perturbation parameters: The threshold voltage and maximum current grow as the perturbation's height and width in the doping density profile increase. When the condition $h\times w = \text{const}$ corresponding to the invariability of the perturbation profile integral is met, the current characteristics remain virtually invariable at different perturbation parameters.

ACKNOWLEDGMENTS

This work was supported by the Russian Foundation for Basic Research, project nos. 16-32-60059 and 16-32-80125.

REFERENCES

1. Shik, A.Ya., *Fiz. Tekh. Poluprovodn. (S.-Peterburg)*, 1974, vol. 8, p. 1841.
2. Wacker, A., *Phys. Rep.*, 2002, vol. 357, p. 1.
3. Keldysh, L.V., *Fiz. Tverd. Tela*, 1962, vol. 4, p. 2265.
4. Esaki, L. and Tsu, R., *IBM J. Res. Dev.*, 1970, vol. 14, 1 p. 61.
5. Scheuerer, R., Schomburg, E., Renk, K.F., et al., *Appl. Phys. Lett.*, 2002, vol. 81, p. 1515.
6. Eisele, H., Khanna, S.P., and Lineld, E.H., *Appl. Phys. Lett.*, 2010, vol. 96, p. 072101.
7. Bonilla, L.L. and Grahn, H.T., *Rep. Prog. Phys.*, 2005, vol. 68, p. 577.
8. Fromhold, T.M., Patane, A., Bujkiewicz, S., et al., *Nature*, 2004, vol. 428, p. 726.
9. Selskii, A.O., Koronovskii, A.A., Hramov, A.E., et al., *Phys. Rev. B*, 2011, vol. 84, p. 235311.
10. Bonilla, L.L. and Teitsworth, S.W., *Nonlinear Wave Methods for Charge Transport*, Weinheim: Wiley, 2010.
11. Hramov, A.E., Makarov, V.V., Koronovskii, A.A., et al., *Phys. Rev. Lett.*, 2014, vol. 112, p. 116603.
12. Maksimenko, V.A., Makarov, V.V., Koronovskii, A.A., et al., *Europhys. Lett.*, 2015, vol. 109, p. 47007.
13. Wacker, A., Schwarz, G., Prengel, F., et al., *Phys. Rev. B*, 1995, vol. 52, p. 13788.
14. Patra, M., Schwarz, G., and Scholl, E., *Phys. Rev. B*, 1998, vol. 57, p. 1824.

Translated by E. Bondareva

SPELL: 1. ok